

# An Allosteric Inhibitor of Protein Arginine Methyltransferase 3

Alena Siarheyeva,<sup>1</sup> Guillermo Senisterra,<sup>1</sup> Abdellah Allali-Hassani,<sup>1</sup> Aiping Dong,<sup>1</sup> Elena Dobrovetsky,<sup>1</sup> Gregory A. Wasney,<sup>1</sup> Irene Chau,<sup>1</sup> Richard Marcellus,<sup>2</sup> Taraneh Hajian,<sup>1</sup> Feng Liu,<sup>3</sup> Ilia Korboukh,<sup>3</sup> David Smil,<sup>1</sup> Yuri Bolshan,<sup>1</sup> Jinrong Min,<sup>1</sup> Hong Wu,<sup>1</sup> Hong Zeng,<sup>1</sup> Peter Loppnau,<sup>1</sup> Gennadiy Poda,<sup>2</sup> Carly Griffin,<sup>2</sup> Ahmed Aman,<sup>2</sup> Peter J. Brown,<sup>1</sup> Jian Jin,<sup>3</sup> Rima Al-awar,<sup>2</sup> Cheryl H. Arrowsmith,<sup>1,4</sup> Matthieu Schapira,<sup>1,5,\*</sup> and Masoud Vedadi<sup>1,\*</sup>

<sup>1</sup>Structural Genomics Consortium, University of Toronto, 101 College Street, MaRS Centre, South Tower, Toronto, ON M5G 1L7, Canada

<sup>2</sup>Medicinal Chemistry Platform, Ontario Institute for Cancer Research, 101 College Street, MaRS Centre, South Tower, Toronto, ON M5G 0A3, Canada

<sup>3</sup>Center for Integrative Chemical Biology and Drug Discovery, UNC Eshelman School of Pharmacy, University of North Carolina at Chapel Hill, Chapel Hill, NC 27599, USA

<sup>4</sup>Ontario Cancer Institute and Department of Medical Biophysics, University of Toronto, ON M5G 2M9, Canada

<sup>5</sup>Department of Pharmacology and Toxicology, University of Toronto, Toronto, ON M5S 1A8, Canada

\*Correspondence: [matthieu.schapira@utoronto.ca](mailto:matthieu.schapira@utoronto.ca) (M.S.), [mvedadi@uhnres.utoronto.ca](mailto:mvedadi@uhnres.utoronto.ca) (M.V.)

<http://dx.doi.org/10.1016/j.str.2012.06.001>

## SUMMARY

PRMT3, a protein arginine methyltransferase, has been shown to influence ribosomal biosynthesis by catalyzing the dimethylation of the 40S ribosomal protein S2. Although PRMT3 has been reported to be a cytosolic protein, it has been shown to methylate histone H4 peptide (H4 1–24) *in vitro*. Here, we report the identification of a PRMT3 inhibitor (1-(benzo[d][1,2,3]thiadiazol-6-yl)-3-(2-cyclohexenylethyl)urea; compound 1) with IC<sub>50</sub> value of 2.5 μM by screening a library of 16,000 compounds using H4 (1–24) peptide as a substrate. The crystal structure of PRMT3 in complex with compound 1 as well as kinetic analysis reveals an allosteric mechanism of inhibition. Mutating PRMT3 residues within the allosteric site or using compound 1 analogs that disrupt interactions with allosteric site residues both abrogated binding and inhibitory activity. These data demonstrate an allosteric mechanism for inhibition of protein arginine methyltransferases, an emerging class of therapeutic targets.

## INTRODUCTION

Epigenetic regulation of gene expression, including mechanisms dependent on histone methylation, have been implicated in a variety of diseases including cancer (Albert and Helin, 2010; Kelly et al., 2010; Nimura et al., 2010; Vallance and Leiper, 2004; Yoshimatsu et al., 2011). Protein lysine (PKMT) and protein arginine (PRMT) methyltransferases catalyze the transfer of a methyl group from S-adenosyl-L-methionine (SAM) to lysine or arginine residues on histone tails, respectively, and in many cases also methylate non-histone proteins (Dhayalan et al., 2011; Huang et al., 2010; Liu et al., 2011; Pagans et al., 2010; Shi et al., 2007). These two families of proteins are distinguishable by the primary sequence of their catalytic domains and

three-dimensional structures (Campagna-Slater et al., 2011; Copeland et al., 2009). Nine different human protein arginine methyltransferases (PRMTs) have been identified and classified into different subtypes. Type I PRMTs, such as PRMT1, PRMT2, PRMT3, PRMT4 (CARM1), PRMT6, and PRMT8, transfer two methyl groups to a single nitrogen atom of the guanidine moiety of arginine (asymmetric dimethylation). Type II PRMTs, such as PRMT5, transfer two methyl groups to two different nitrogen atoms of the guanidine (symmetric dimethylation). PRMT7 was found to monomethylate various substrates (Bedford and Richard, 2005; Di Lorenzo and Bedford, 2011) and recently, Zurita-Lopez et al. confirmed that PRMT7 only monomethylates its substrates and it is not capable of catalyzing dimethylation (a type III enzyme) (Zurita-Lopez et al., 2012). Arginine residues 2, 8, 17, and 26 of histone H3 and arginine 3 of H4 are substrates for PRMTs.

PRMT3 is a type I PRMT and has been shown to be a cytosolic protein. A 29 kDa protein was originally reported as a substrate for PRMT3 (Tang et al., 1998), which was later identified as 40S ribosomal protein S2 (rpS2) in yeast (Bachand and Silver, 2004) and mammalian cells (Swiercz et al., 2005). PRMT3 methylates rpS2, resulting in stabilization, and plays a role in proper maturation of the 80S ribosome (Bachand and Silver, 2004; Di Lorenzo and Bedford, 2011; Swiercz et al., 2005). Methylation of rpS2 is conserved from yeast to human and influences ribosomal biosynthesis while pre-rRNA processing occurs normally (Bachand and Silver, 2004; Swiercz et al., 2005, 2007). Cells lacking PRMT3 have been reported to show accumulation of free 60S ribosomal subunits and an imbalance in the 40S:60S free subunit ratio. PRMT1 and PRMT3 have been reported to methylate the recombinant mammalian nuclear poly(A)-binding protein (PABPN1) which carries 13 asymmetrically dimethylated arginine residues in its C-terminal domain (Fronz et al., 2008; Smith et al., 1999; Tavanez et al., 2009). PRMT3 function has been reported to be essential for dendritic spine maturation in rats (Miyata et al., 2010). It also methylates a histone peptide (H4 1–24) *in vitro* (Allali-Hassani et al., 2011). Histone H4R3 is a modification associated with an increase in transcription of a number of genes, including those under control of estrogen receptor  $\alpha$  and androgen receptor (Herrmann et al., 2009;

Obiany et al., 2011; Wagner et al., 2006). Interestingly, the tumor suppressor DAL-1/4.1B interacts with PRMT3 and inhibits its protein arginine methyltransferase activity, suggesting that DAL-1/4.1B may affect tumor growth by regulating protein arginine methylation (Singh et al., 2004).

The critical roles of protein methyltransferases (PMTs) in a variety of biological processes (Guccione et al., 2007; Hyllus et al., 2007; Iberg et al., 2008; Pawlak et al., 2000; Yadav et al., 2003) and diseases suggest that many of these enzymes may be targets for a new generation of therapeutics (Fietze et al., 2008; Hong et al., 2004; Kelly et al., 2010; Richon et al., 2011). Within the last few years, efforts to identify inhibitors of PRMTs have led to the identification of a number of compounds with low or submicromolar  $IC_{50}$  values for CARM1 and PRMT1 (Allan et al., 2009; Bissinger et al., 2011; Cheng et al., 2011; Huynh et al., 2009; Obiany et al., 2011; Purandare et al., 2008; Therrien et al., 2009; Wan et al., 2009). CARM1 has been shown to be upregulated during the progression of prostate cancer (Hong et al., 2004) and in breast tumors (El Messaoudi et al., 2006). PRMT1 and PRMT3 are overexpressed in human myocardial tissues from patients with coronary disease (Chen et al., 2006) and have been implicated in oculopharyngeal muscular dystrophy (OPMD) (Tavanez et al., 2009). Polyalanine expansion in PABPN1 causes OPMD (Brais et al., 1998). PRMT1 and PRMT3 are reported to be more associated with expanded PABPN1 than normal PABPN1 and are found in intranuclear inclusions formed by deposition of PABPN1 fibrils (Tavanez et al., 2009). Here, we report the discovery of 1-(benzo[d][1,2,3]thiadiazol-6-yl)-3-(2-cyclohexenylethyl)urea (compound **1**), a selective allosteric inhibitor of PRMT3, suggesting a possible novel mechanism for targeting PRMTs in general. The structure of PRMT3 in complex with compound **1** along with characterization of PRMT3 mutants reveals the mechanism of selective allosteric inhibition and will be useful in further development of more potent and cell active PRMT3 inhibitors.

## RESULTS

### Identification of Compound **1** as a PRMT3 Inhibitor

To identify inhibitors of PRMT3 activity, we screened truncated PRMT3 (residues 211–531) against a library of sixteen thousand diverse drug-like compounds (Supplemental Experimental Procedures) using a histone peptide (histone 4, residues 1–24) as a substrate. The primary screen was performed using a SAHH (S-adenosylhomocysteine hydrolase)-coupled assay (Allali-Hassani et al., 2011) at peptide and SAM concentrations of 2- and 5-fold above the  $K_m$  for each substrate, respectively. The most potent hit, compound **1** (1-(benzo[d][1,2,3]thiadiazol-6-yl)-3-(2-cyclohexenylethyl)urea), had an  $IC_{50}$  value of  $2.5 \pm 0.1 \mu\text{M}$  (Hill Slope of 1.5) at peptide and SAM concentrations equivalent to their respective  $K_m$  values (Figure 1). Compound **1** also inhibited the commercially available full length PRMT3 with an  $IC_{50}$  value of  $1.6 \pm 0.3 \mu\text{M}$  (Hill Slope of 0.99; Figure S1 available online). Compound **1** had no inhibitory effect on SAHH activity, or other components of the assay and direct binding of compound **1** to PRMT3 was confirmed by surface plasmon resonance (SPR) (Figure 2). Compound **1** exhibited rapid on and off rates with a  $K_D$  value of  $9.5 \pm 0.5 \mu\text{M}$  as determined by steady state analysis. In similar experiments the pres-

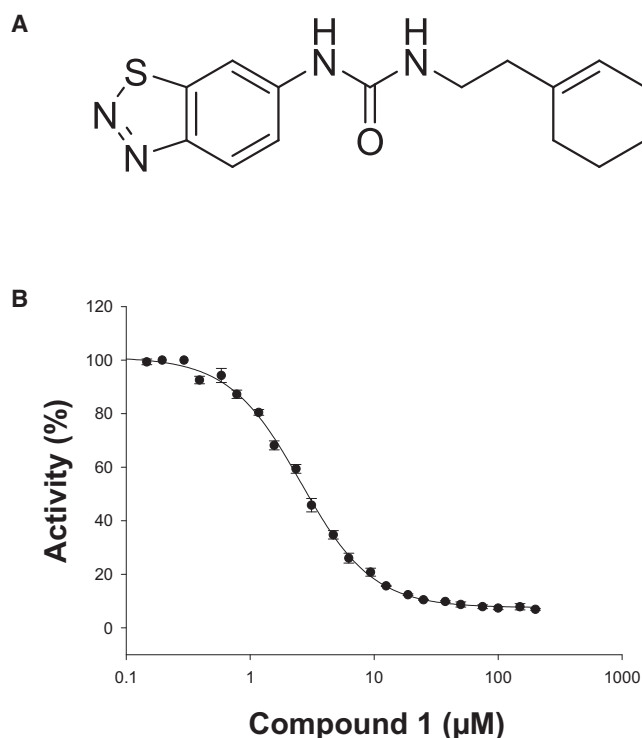


**Figure 1. Compound **1** Is a Potent Inhibitor of PRMT3 Activity**

(A) Crystal structure of compound **1** was determined and indicated that the compound is 1-(benzo[d][1,2,3]thiadiazol-6-yl)-3-(2-cyclohexenylethyl)urea. (B) Compound **1** inhibits the activity of PRMT3 at a balanced condition with  $IC_{50}$  of  $2.5 \pm 0.1 \mu\text{M}$  as determined by SAHH-coupled assay. See also Figures S1 and S2 and Table S2. Data points are presented as mean values  $\pm$  SD from three experiments.

ence of  $100 \mu\text{M}$  SAM did not affect the  $K_D$  value of compound **1** ( $7 \pm 0.7 \mu\text{M}$ ).  $K_D$  values for SAM in the presence of  $20 \mu\text{M}$  and absence of compound **1** ( $55 \pm 0.8$  and  $59 \pm 7 \mu\text{M}$ , respectively) were not significantly different either, indicating that SAM and compound **1** are not competing for binding to PRMT3. Kinetic analysis indicated that compound **1** is a noncompetitive inhibitor of PRMT3 activity with respect to both SAM and peptide substrates with  $K_i$  values of  $2.9 \pm 0.1$  and  $4.2 \pm 1.1 \mu\text{M}$ , respectively (Figure 3). We also assessed the inhibitory effect of compound **1** on activity of PRMT3 using rpS2 as a substrate. We expressed and purified recombinant rpS2 and determined the kinetic parameters (Figures 4A and 4B). PRMT3 catalyzed the methylation of rpS2 with a  $k_{\text{cat}}$  value of  $0.1 \text{ min}^{-1}$  and  $K_m$  values of  $1 \pm 0.5 \mu\text{M}$  and  $34 \pm 1 \mu\text{M}$  for rpS2 and SAM, respectively. The activity of PRMT3 was linear at the  $K_m$  of both substrates (Figure 4C) and was inhibited by compound **1** with an  $IC_{50}$  value similar to that determined for the histone substrate ( $2 \pm 0.5 \mu\text{M}$ ; Figure 4D).

Selectivity of compound **1** for PRMT3 was assessed by screening against protein lysine methyltransferases G9a, EHMT1, SUV39H2, SETD7, and SETD8 using the same SAHH-coupled assay and protein arginine methyltransferases PRMT1, PRMT4, PRMT5, and PRMT8 using a radioactivity-based assay (Figure S2). Inhibition of the full-length PRMT3 was also performed using the radioactivity-based as described

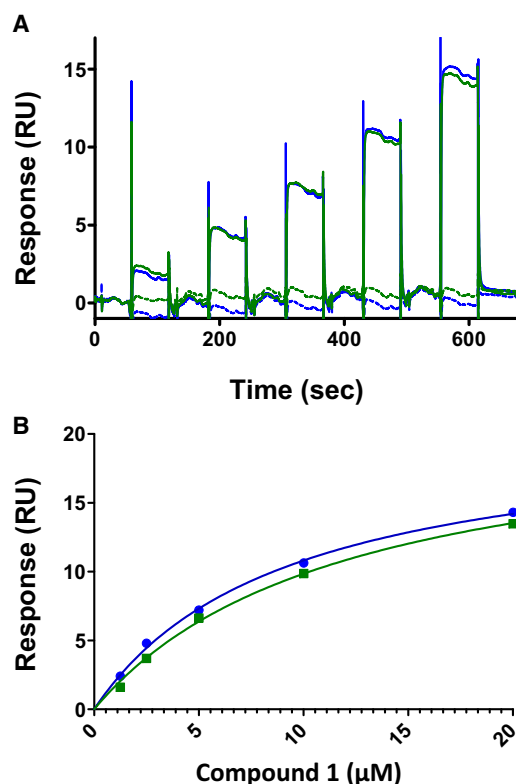


**Figure 2. Binding of Compound 1 Was Confirmed by SPR**

(A) The subtracted sensorgram (fc3-fc1) of the duplicate compound 1 samples showing blanks and compound cycles from a Biacore T200 single cycle kinetic run. The compound concentrations are 1.25, 2.5, 5, 10, and 20 μM, with 60 s on and off times.

(B) The duplicate binding curves that were used to calculate the  $K_D$  and  $R_{Max}$  values for the compound 1-PRMT3 interaction are shown.

in the material and methods. All reactions were performed in the linear range at substrate and SAM concentrations equivalent to their respective  $K_m$  values for each enzyme. Compound 1 showed no inhibitory activity on any of the PKMTs, which have a very different overall protein conformational fold compared to the PRMTs. Similarly, PRMT1, PRMT4, or PRMT8 (those closest in sequence to PRMT3; 35%–51% amino acid sequence identity) were not inhibited by compound 1, while PRMT5 was very weakly inhibited. In addition, we cannot rule out the possibility of inhibition against more distantly related methyltransferases (<20% sequence identity), such as SPOUT RNA methyltransferases (Petrossian and Clarke, 2011).

#### Compound 1 Binds in a Novel PRMT-Specific Allosteric Pocket

To better understand the mechanism of action of compound 1, the compound was cocrystallized with PRMT3 and the structure was determined to 2.0 Å resolution (PDB ID: 3SMQ; Table 1). The complex structure revealed that the compound binds in a pocket distinct from both the SAM and substrate peptide binding pockets. Inhibitor-bound PRMT3 adopts a canonical PRMT dimeric structure, previously described for rat PRMT3, PRMT1, and CARM1 (Troffer-Charlier et al., 2007; Yue et al., 2007; Zhang

and Cheng, 2003; Zhang et al., 2000) (Figure S3): each monomer is composed of a cofactor binding domain structurally related to the SAM-dependent methyltransferase fold, a barrel-like domain that may contribute to recruitment of substrate, and a helical dimerization arm that interacts with the alpha-Y segment of the activation helix of the opposite subunit (Figure 5A). The structure is very similar to that of cofactor-bound PRMT3 (PDB code 2FYT, RMSD: 0.98 Å), with three important differences: (1) the inhibitor is partially nested in a pocket which is absent from the cofactor-bound structure, and located at the base of the dimerization arm (here on referred to as “the allosteric pocket”); (2) the alpha-X segment of the activation helix, that was shown to be critical for catalytic activity of PRMT1 and CARM1 (Troffer-Charlier et al., 2007; Zhang and Cheng, 2003) is disordered; (3) the cofactor is missing (Figure 5A and Figure S3).

Compound 1 binds to PRMT3 at the dimer interface. Three structural features characterize the interaction: First, the benzothiadiazole moiety fits tightly in the allosteric pocket, and forms a hydrogen bond with the side chain of T466. Second, the urea linker is located at the entrance of the cavity, and forms hydrogen bonds with the guanidinium of R396 and the carboxylate of E422. Third, the cyclohexyl arm extends out of the allosteric pocket and makes hydrophobic interactions with a surface composed of the side chains of R396 and E248 from two different monomers (Figure 5B).

Importantly, in the structure of the same PRMT3 construct bound to SAH, the side chain of R396 interacted with E422 of the same subunit, resulting in complete obstruction of the allosteric pocket (PDB code 2FYT) (Figure 5B; left panel). Compound 1 binding induces flipping of R396 out of the pocket. This motion is accompanied by a structural rearrangement of Y244 of the alpha-Y segment of the activation helix, and loss of electron density for the alpha-X segment, which apparently becomes disordered (Figures 5B and 5C). It is not clear from our data whether ligand binding and apparent destabilization of alpha-X are linked or fortuitous, but we note that (1) the necessary flipping of R396 is not compatible with the conformation of Y244 observed in the cofactor-bound structure (PDB code 2FYT), (2) Y244 is positioned at the junction of alpha-X and alpha-Y segments, and (3) proper folding of alpha-X onto the cofactor is required for the enzymatic activity of PRMT1 and CARM1 (Troffer-Charlier et al., 2007; Zhang and Cheng, 2003). Analytical ultracentrifugation data indicated that PRMT3 is a dimer in solution in the presence and absence of the compound (Supplemental Experimental Procedures).

#### Site-Directed Mutagenesis

To investigate the mechanism of inhibition of PRMT3 by compound 1, we mutated residues involved in compound binding (K392, V420, E422, and T466) and dimerization (W400) (Table 2). We also mutated R396, which is involved in both compound binding and dimerization in the inhibitor-bound conformation, but not in the cofactor-bound form. In order to distinguish mutations that globally destabilized the protein, we measured the thermal stability and in vitro half-life of each mutant. Mutation of R396, W400, E422, and T466 all had global effects on protein stability, indicating the importance of both dimerization and residues of the allosteric pocket to the overall fold and activity of PRMT3. The other three mutants had

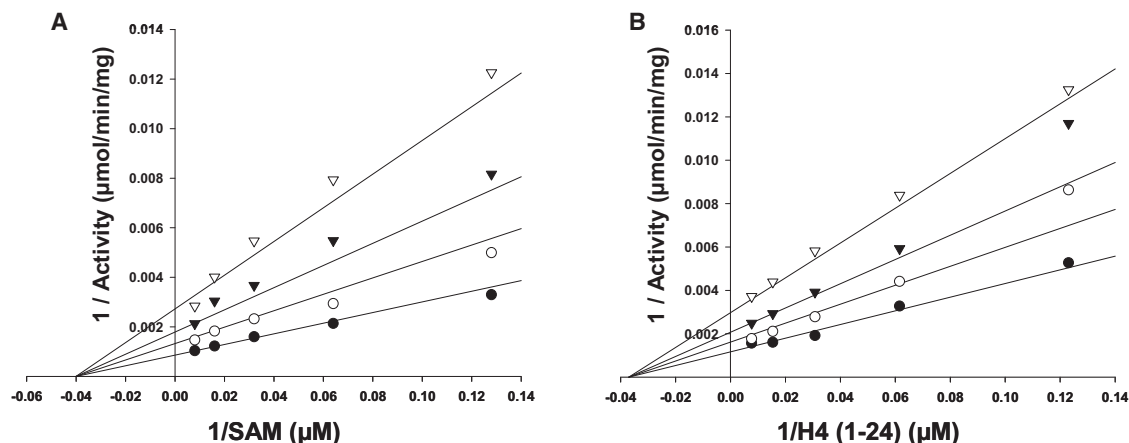


**Figure 3. Kinetic Analysis of Compound 1 Inhibition of PRMT3 Activity**

Lineweaver-Burk plots for kinetic analysis of compound 1 inhibition by SAHH-coupled assay at varying concentrations of (A) SAM and (B) H4 (1–24) peptide are shown at 0 (●), 1.5 (○), 3 (▼), and 6 (▽) μM of compound 1.

interesting activities that support our analysis of the mode of action of compound 1. The V420W mutant was designed to mimic the action of the inhibitor by occupying the allosteric pocket and forcing R396 to flip out of the pocket (Figures 5B and 5D). This mutant had significantly reduced catalytic efficiency (5,400 versus 65,400  $\text{M}^{-1} \text{min}^{-1}$ ) and increased the  $\text{IC}_{50}$  value for the compound by an order of magnitude (Table 2; Figure 6). Second, mutation of K392 to either Arg or Ala would be expected to antagonize the binding of compound 1 by recruiting E422 away from the inhibitor or opening the binding pocket to solvent, respectively (Figure 5D). Indeed compound 1 displayed approximately 5-fold weaker inhibition with these two mutants compared to wild-type protein (Table 2; Figure 6). These results show that mutants mimicking the action of compound 1 at the allosteric site inhibit PRMT3, and mutants preventing compound 1 from binding at the allosteric site neutralize the compound's ability to inhibit the enzyme.

Several lines of evidence clearly indicate that the conformation of helix  $\alpha$ -X controls the enzymatic activity of PRMTs. First,  $\alpha$ -X folds like a lid on the cofactor (Figure 5C and Figure S3), which allows interaction between a conserved tyrosine of the helix with a catalytic glutamate (Y241 and E355 in PRMT3, respectively), in a conformation necessary for proper positioning of the substrate arginine (Troffer-Charlier et al., 2007; Yue et al., 2007). A very specific positioning of  $\alpha$ -X is therefore necessary for the formation of a catalytically competent active site. Second,  $\alpha$ -X is disordered in all PRMT structures where the cofactor is missing while it is folded on the cofactor in structures of CARM1 and PRMT3 almost in all structures where the cofactor is present (Figure S3) (Troffer-Charlier et al., 2007; Yue et al., 2007; Zhang et al., 2000). Third, deletion of  $\alpha$ -X from rat PRMT1 reduced cofactor binding and abolished enzymatic activity (Zhang and Cheng, 2003). We have shown that binding of compound 1 induces conformational side-chain rearrangements at the junction of  $\alpha$ -Y and  $\alpha$ -X helices and is accompanied by destabilization of helix  $\alpha$ -X (Figures 5B and 5C). It is possible that this chain of events is causative and underlies the mechanism of allosteric inhibition. It is also

possible that binding of compound 1 at the allosteric site prevents positioning of the substrate peptide in a catalytically competent conformation.

#### Structure-Activity Relationship Confirms that Binding at the Allosteric Site Mediates Inhibition

To further confirm the conformation of compound 1 within the allosteric binding pocket of PRMT3 and to test the features of the compound required for binding and inhibition, we carried out structure-activity relationship (SAR) studies as a complementary approach to site-directed mutagenesis. We first examined whether the uncommon cyclohexenylethyl group was absolutely needed for the inhibitory activity. As expected, this uncommon group could indeed be replaced by a more common group, the cyclohexylethyl group, without any potency loss and the alkene functionality was unnecessary (compound 1 versus compound 2, Table 3). On the other hand, the replacement of the cyclohexenylethyl (compound 1) or cyclohexylethyl group (compound 2) with the benzyl group (compound 5) led to almost 10-fold loss of potency. We then designed and synthesized the other compounds outlined in Table 3 to probe hydrogen-bond interactions of compound 1 with the allosteric binding pocket of PRMT3. Replacing the benzothiadiazole moiety (compound 2) with the corresponding benzothiazole moiety (compound 3) resulted in > 50-fold loss of potency, suggesting that the hydrogen-bond interaction between the middle nitrogen of benzothiadiazole moiety and T466 is critical for binding. N-methylation of either nitrogen of the urea moiety led to complete loss of potency (>50-fold potency loss for compound 4 versus compound 2; >5-fold potency loss for compound 7 versus compound 5), which suggests that the hydrogen-bond interactions between the urea moiety and E422 are important. In addition, compound 6, a thiourea designed to probe the hydrogen-bond interaction between the oxygen of the urea moiety and R396, was over 5-fold less potent than its urea analog, compound 5. These data clearly show that hydrogen-bond interactions observed in the crystal structures that are key for binding at the allosteric site are also critical for inhibition. Taken

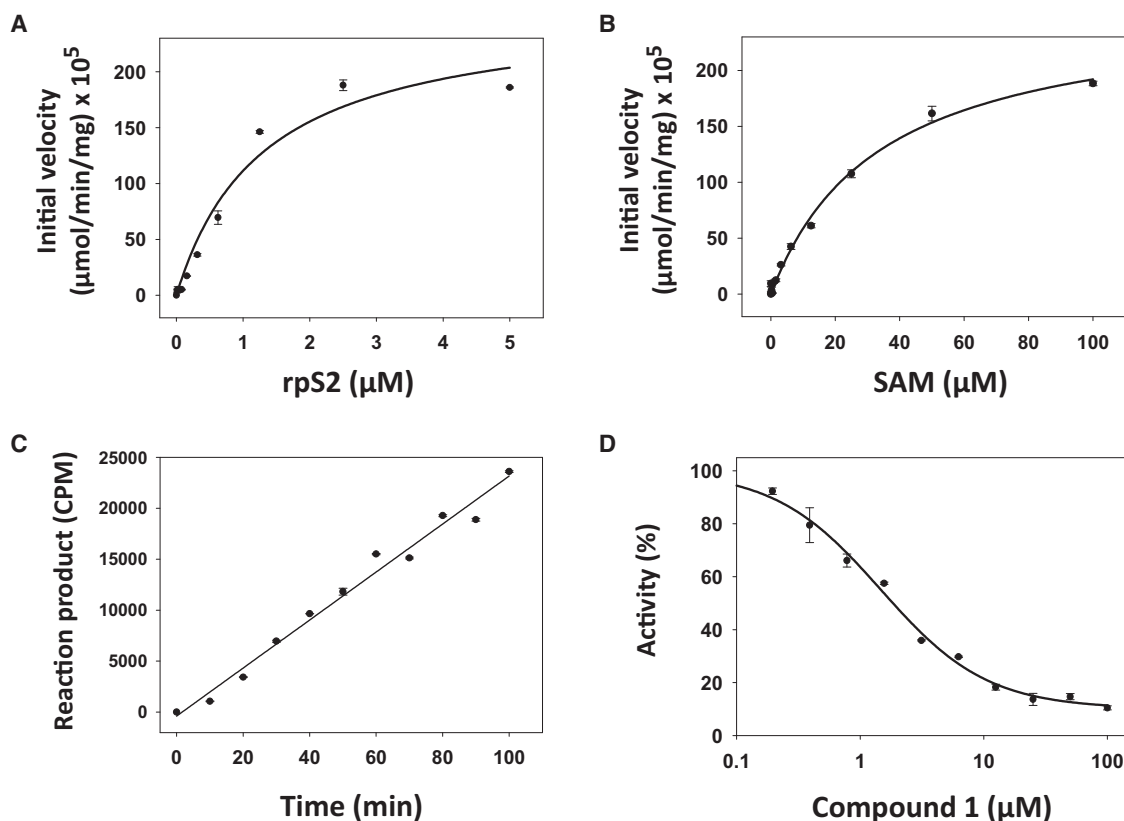


**Figure 4. PRMT3 Activity Using rpS2 as a Substrate**

$K_m$  values were determined for (A) rpS2 ( $1 \pm 0.5 \mu\text{M}$ ) and (B) SAM ( $34 \pm 1 \mu\text{M}$ ) with a  $k_{\text{cat}}$  value of  $0.1 \text{ min}^{-1}$  using a radioactivity based assay as described in the material and method. (C) Activity of PRMT3 was linear at  $K_m$  of both substrates and (D) was inhibited by compound **1** with an  $\text{IC}_{50}$  value of  $2 \pm 0.5 \mu\text{M}$ . Data points are presented as mean values  $\pm$  SD from three experiments.

together, these results and our mutational analysis strongly support an allosteric mechanism for PRMT3 inhibition.

#### Bioavailability of Compound 1

In order to determine cell permeability of compound **1**, we conducted Caco2 permeability and efflux assay as described in the Supplemental Experimental Procedures. This is an in vitro assay to test for intestinal absorption and efflux of compounds that can also be used as an indication of cell permeability (Artursson, 1990; Yee, 1997). Compound **1** was tested at 10 and 20  $\mu\text{M}$  in triplicate along with metoprolol (a positive control with high permeability and low efflux), atenolol (low permeability) and digoxin (with low permeability and high efflux). The data for all controls were reproducible and compound **1** showed high permeability and negative efflux indicating it is cell permeable (Table S1). However, unlike the controls, post-assay recovery of compound **1** was only 32% at 20  $\mu\text{M}$  suggesting the compound may have been metabolized or precipitated during the assay period. To assess whether the compound is likely to be metabolized, it was subjected to a liver microsome assay (Supplemental Experimental Procedures). Liver microsome stability is typically used as an in vitro model of first-pass metabolism, but we are only using it here as an indicator of metabolic liability in any cellular system including Caco2 that contains metabolizing enzymes, such as cytochrome P450s (Engman

et al., 2001; Meyer et al., 2007; Swanson, 2004). Testosterone and propranolol were used as controls. These compounds are expected to be significantly metabolized in this system within 30 min. Antipyrine on the other hand is expected to be stable within the same timeline. All controls worked as expected (Table S2). Compound **1** was assayed in triplicate using both human and mouse liver microsomes. The percent remaining for compound **1** was only about 8% indicating that this compound may not be stable enough for cell-based assays. Generating more stable analogs may provide better tools for follow-up experiments.

#### DISCUSSION

By screening a diverse library of drug-like compounds, we have identified compound **1** as a selective PRMT3 inhibitor. Enzyme kinetics, cocrystal structure of the complex, mutational analysis, and structure-activity relationship all indicate that PRMT3 inhibition is mediated by binding at a previously unknown allosteric site.

Clinical approval of HDAC and DNA methyltransferase inhibitors for treatment of hematological malignancies has resulted in a growing interest in chemical regulation of chromatin mediated signaling. Consequently, a number of potent and selective inhibitors targeting PMTs have recently been reported (Yost

**Table 1. Data Collection and Refinement Statistics of the PRMT3-Compound 1 Cocrystal Structure—Molecular Replacement**

3SMQ	
Data Collection	
Space group	P4 <sub>3</sub> 2 <sub>1</sub> 2
Cell dimensions	
<i>a</i> , <i>b</i> , <i>c</i> (Å)	70.65, 70.65, 171.98
$\alpha$ , $\beta$ , $\gamma$ (°)	90.00, 90.00, 90.00
Resolution (Å)	50.00–2.00(2.03–2.00)
<i>R</i> <sub>sym</sub> or <i>R</i> <sub>merge</sub>	0.078 (0.558)
<i>I</i> / $\sigma$ <i>I</i>	36.61 (2.17)
Completeness (%)	98.1 (83.4)
Redundancy	11.5 (6.0)
Refinement	
Resolution (Å)	50.00–2.00
No. reflections	28,754
<i>R</i> <sub>work</sub> / <i>R</i> <sub>free</sub>	0.190/0.215
No. atoms	
Protein	2,374
Ligand/ion	21
Cholide	1
Water	226
<i>B</i> factors	
Protein	29.1
Ligand/ion	33.0
Water	41.1
Rmsds	
Bond lengths (Å)	0.010
Bond angles (°)	1.214

et al., 2011). For example, new peptide-competitive inhibitors have been reported for the PKMTs G9a (Vedadi et al., 2011) and SMYD2 (Ferguson et al., 2011) as well as PRMT CARM1 (Sack et al., 2011), and a cofactor-competitive inhibitor was recently reported for DOT1L (Daigle et al., 2011). To our knowledge, no allosteric inhibitor has yet been reported for any writer, reader or eraser of methyl marks. We believe that the discovery of compound **1** stands as a proof-of-concept for allosteric inhibition of PRMTs: a pocket is present at the same position in cofactor-bound PRMT1 (PDB code 1ORI) and a narrow channel can be seen in *apo* CARM1 (PDB code 3B3J) that may be able to accommodate small molecule ligands upon side-chain motion. It is therefore reasonable to speculate that the allosteric mechanism described here may apply to PRMTs in general. The structures of PRMTs are dramatically different from those of PKMTs, in that PKMTs have an unrelated topology and are active as monomers. The allosteric site that we have identified has therefore no equivalent in PKMTs, and it is highly improbable that compounds binding at this site would inhibit PKMTs. The allosteric mechanism uncovered is therefore PRMT specific.

PRMTs are ubiquitously expressed, essential for embryogenesis (Pawlak et al., 2000; Yadav et al., 2003) and regulate gene expression (Guccione et al., 2007; Hyllus et al., 2007; Iberg

et al., 2008). PRMT3 has been implicated in a variety of biological processes including methylation of rpS2, PABPN1, and interaction with DAL-1/4.1B tumor suppressor. Increase in its activity or level of expression may also contribute to coronary heart disease: in normal vascular physiology, endothelium-derived nitric oxide (NO) is one of the most potent endogenous vasodilators and is known as an endogenous vasoprotective agent in diabetes (Colasanti and Suzuki, 2000; Groop et al., 2005; Mariotto et al., 2004; Yamagishi and Matsui, 2011). NO is synthesized from L-arginine via the action of NO synthase (NOS) (Yamagishi and Matsui, 2011). Endogenous L-arginine analogs such as asymmetric dimethylarginine (ADMA) inhibit NOS. ADMA is not derived from the methylation of free arginine, rather it is produced during catabolism of proteins with asymmetric dimethylated arginine (Kielstein et al., 2001a, 2001b; Vallance and Leiper, 2004). Plasma levels of ADMA are elevated in patients with vascular disease (Kielstein et al., 2001a) and so are PRMT1 and PRMT3 expression levels in myocardial tissue from patients with atherosclerosis (Chen et al., 2006), implicating PRMT3 in regulation of NOS activity and related diseases. Thus, further optimization of compound **1** should result in the generation of chemical tools to probe the relevance of PRMT3 as a therapeutic target in vascular and related diseases.

## EXPERIMENTAL PROCEDURES

### Material

A sixteen thousand diverse, commercial library of drug-like compounds was screened to identify compound **1** whereas the rest of the compounds were synthetically prepared (see the Supplemental Experimental Procedures for details).

Adenosine deaminase (ADA) was purchased from Sigma (Cat. no. 096K7003; <http://www.sigmaldrich.com>), ThioGlo from Calbiochem (Cat. no. 595501; <http://www.emdchemicals.com>) and SAH (S-adenosine homocysteine) from Sigma (Cat. no. A9384). 384-well plates were purchased from Axygen (Cat. no. PCR-384-BK; <http://www.axxygen.com>) and Greiner (Cat. no. 784209; <http://www.greinerbioone.com>). 96-well plates were obtained from Nalgene (Cat. no. 249944; <http://www.nalgenelabware.com>). Histone 4 (H4 [1–24], SGRGKGGKGLGKGGAKRHRKVLDR) and histone 3 (H3 [1–25], ARTKQTARKSTGGKAPRQLATKAA) were purchased from Tufts University. Full-length human, recombinant, N-terminal GST tagged PRMT3 was purchased from BPS Bioscience (Cat. no. BPS-51043, Lot no. 110111).

### Cloning of PRMT3 Mutants

All PRMT3 mutants were generated by site-directed mutagenesis. Primers that spanned the altered codons with sizes ranging from 29 to 58 bp were designed using the “Quikchange Primer Design” program (<http://www.genomics.agilent.com>). The wild-type PRMT3 gene (amino acids 211–531) was cloned into the pET28a-LIC vector (GenBank EF442785), expressed and purified as previously reported (Wu et al., 2010). PRMT3 DNA was then PCR-amplified using Pfu Ultra II (Stratagene) with the designed primers according to the manufacturer's protocol (<http://www.genomics.agilent.com/files/Manual/200523.pdf>). The PCR products were digested with DpnI for 1 hr at 37°C, and transformed into DH5 $\alpha$  cells. The cells were plated on Luria broth (LB) plates supplemented with 50  $\mu$ g/ml kanamycin and incubated overnight at 37°C. Three colonies were chosen from each plate, inoculated into 3 ml of LB (with kanamycin), and incubated overnight at 37°C with shaking. DNA was purified from each cell pellet using the QIAprep Spin MiniPrep Kit (QIAGEN). All mutations were confirmed by sequencing (ACGT).

### Expression and Purification of PRMT3 Mutants and rpS2

The PRMT3 mutant constructs and rpS2 construct (GST-rpS2; a generous gift from Dr. Mark Bedford) were expressed in BL21-V2R-pRARE-2 cells

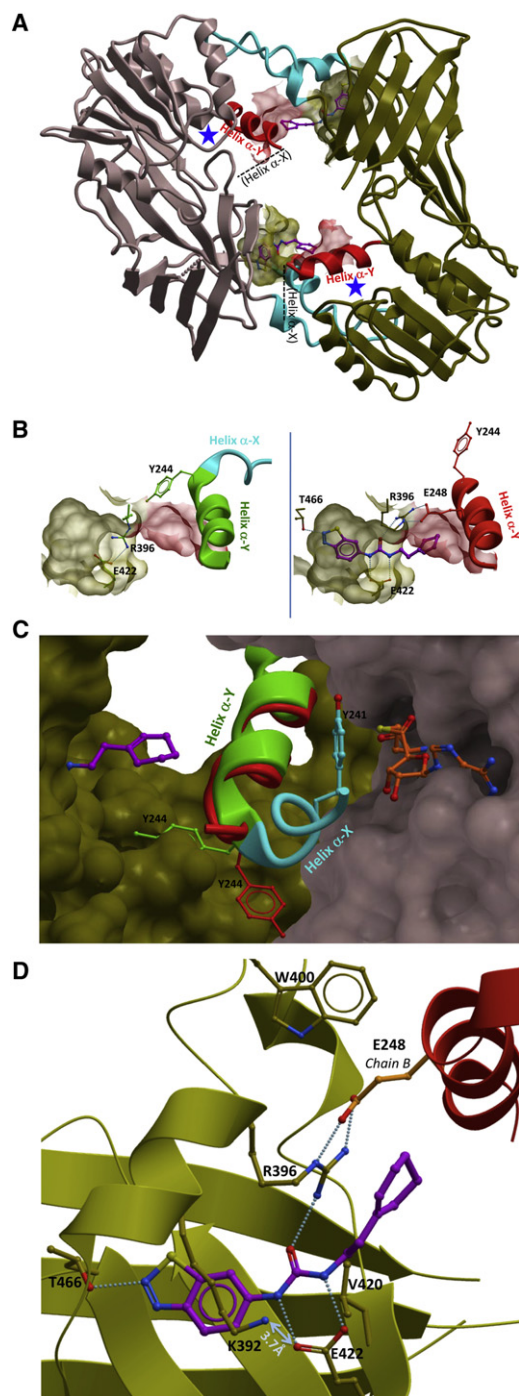


**Figure 5. Structural Analysis of Compound 1 Binding**

(A) Overall structure. The PRMT3 catalytic core adopts a canonical PRMT dimeric structure. The inhibitor (magenta) binds a pocket at the base of the dimerization arm (cyan) of one chain and contacts the alpha-Y segment of the activation helix of the other monomer (red). The alpha-X segment of the activation helix is disordered (dashed line), and the cofactor is absent (blue star: expected position).

(B) Inhibitor binding. In the absence of inhibitor, R396 occupies the binding pocket. Helix alpha-X: cyan; helix alpha-Y: green (left). Inhibitor binding induces consecutive conformational rearrangements of residues at the N-terminus of helix alpha-Y, accompanied by destabilization of helix alpha-X (disordered, right). The thiadiazole end of the compound is deeply buried in

(SGC Toronto) and purified as described in the Supplemental Experimental Procedures.

#### Biochemical Assays

##### SAHH-Coupled Assay

The methyltransferase activities of G9a, SETD7, PRMT3, EHMT1, SETD8, SUV39H2, and PRMT3 mutants were measured using SAHH-coupled assay as described before (Allali-Hassani et al., 2011). In this assay, SAHH and ADA convert the methyltransferase reaction product SAH to homocysteine and inosine. The abundance of homocysteine is quantified using ThioGlo (Calbiochem), which reacts with thiols and fluoresces strongly (Supplemental Experimental Procedures).

##### Scintillation Proximity Assay

Selectivity of compound 1 against PRMT1, PRMT4, PRMT5-MEP50 complex, and PRMT8 was assessed by a radioactivity based assay in parallel with that for full-length (FL) PRMT3. The radioactivity based assay was used as these PRMTs were not amenable to SAHH-coupled assay. In this assay  $^3\text{H}$ -SAM (Cat. no. NET155V250UC, Perkin Elmer) was used as a methyl donor to methylate peptide substrates. Peptide substrates were biotinylated to be captured in each well through their interaction with streptavidin using a streptavidin-coated Flash plate. The amount of the product (methylated peptide) was quantified by tracing the radioactivity (counts per minutes measured by a TopCount reader from Perkin Elmer). Assay conditions were optimized for each protein separately, and all experiments were performed at linear initial velocity. The first 24 residues of histone 4 (H4 [1–24], SGRGKGGKGLGKGGAKRHRKVLDR) was used as a substrate for PRMT1, PRMT3 (FL), PRMT5/MEP50, and PRMT8. The substrate for PRMT4 was 24 residues of histone 3 (H3 [21–44], ATKAARKSAPATGGVKKPHRYRPG). The final concentrations of PRMT1, PRMT3 (FL), PRMT4, PRMT5-MEP50 complex, and PRMT8 in the assay were 20, 350, 270, 500, and 150 nM, respectively. The concentrations of SAM and peptide substrate were set around their respective  $K_m$  values. SAM concentration for PRMT1 and PRMT8 was 10  $\mu\text{M}$ , and for PRMT3 (FL) and PRMT4 was 20  $\mu\text{M}$ . Peptide concentrations for PRMT1, PRMT3 (FL), PRMT4, and PRMT8 were 15, 7, 20, and 15  $\mu\text{M}$ , respectively. For PRMT5/MEP50 complex SAM concentration of 6  $\mu\text{M}$ , and peptide (H4 [1–24]) concentration of 20  $\mu\text{M}$  was used. The reaction was prepared in the final volume of 10  $\mu\text{l}$ . The reaction mix contained 7  $\mu\text{l}$  of buffer (20 mM Tris, 10 mM DTT [pH 8]), 1  $\mu\text{l}$  enzyme, and 1  $\mu\text{l}$  of 66  $\mu\text{M}$   $^3\text{H}$ -SAM (diluted with cold SAM to achieve the desired concentrations of SAM in each assay). The reaction was started by adding 1  $\mu\text{l}$  of a respective peptide substrate. The reaction mixtures were incubated for 60 min for all HMTs except for PRMT5/MEP50 complex, for which the reaction was incubated for 30 min. The reaction was quenched with equal volumes of 7.5 M guanidine-HCl. 10  $\mu\text{l}$  of the reaction mix containing Guanidine-HCl was mixed with 190  $\mu\text{l}$  of 20 mM Tris buffer (pH 8) and transferred into a Flash plate (96-well FlashPlate, Cat. no. SMP103, Perkin Elmer, <http://www.perkinelmer.com/>). The plate was incubated for an hour prior to reading using a TopCount (Perkin Elmer, <http://www.perkinelmer.com/>) to accumulate maximum signal.

##### PRMT3 Activity Assay Using rpS2 as a Substrate

Effect of compound 1 on PRMT3 methylation of its physiological substrate rpS2 was tested using a radioactivity based assay. In this assay  $^3\text{H}$ -SAM (Cat. no. NET155V250UC, Perkin Elmer) was used as a methyl donor to methylate rpS2 substrate. PRMT3 and methylated rpS2 were later precipitated using 10% trichloroacetic acid (TCA) and captured on 96-well Multiscreen Filter Plates (Cat. no. MSFBN6B10, Millipore). The amount of the product

the pocket and is hydrogen bonded to the hydroxyl group of T466; the urea linker is positioned at the entrance of the pocket and forms hydrogen bonds with the side chains of R396 and E422; the cyclohexyl moiety extends out of the pocket, toward the alpha-Y helix of the second monomer (red).

(C) Proposed inhibition mechanism. Compound 1 binding (magenta) induces a conformational rearrangement at the N-terminus of helix alpha-Y (inhibitor present: red, inhibitor absent: green), which destabilizes the active form of helix alpha-X (cyan), critical for enzymatic activity.

(D) Mapping of critical residues at the allosteric site.

See also Figure S3 and Table S1.

**Table 2. Characterization of PRMT3 Mutants**

Protein	$K_m$ ( $\mu\text{M}$ )		$k_{\text{cat}}$ ( $\text{min}^{-1}$ ) $\times 10^2$	$k_{\text{cat}}/K_m$ ( $\text{M}^{-1} \text{min}^{-1}$ )	Compound 1 $\text{IC}_{50}$ ( $\mu\text{M}$ )	t1/2 (min)
	Peptide	SAM				
Wild-type	13 $\pm$ 4	20 $\pm$ 2	85 $\pm$ 10	65400	2.2 $\pm$ 0.1	>300
K392R	16 $\pm$ 2	19 $\pm$ 7	127 $\pm$ 10	79400	12 $\pm$ 1	>300
K392A	12 $\pm$ 2	21 $\pm$ 3	52 $\pm$ 7	43300	9.1 $\pm$ 0.4	>300
V420W	33 $\pm$ 0.4	33 $\pm$ 10	18 $\pm$ 7	5400	23 $\pm$ 1	>300
E422A	Not stable	Not stable	Not stable	Not stable	NA	>300
T466A	Not stable	Not stable	Not stable	Not stable	NA	36 $\pm$ 6
T466V	Inactive	Inactive	Inactive	Inactive	NA	38 $\pm$ 1
R396N	Inactive	Inactive	Inactive	Inactive	NA	44 $\pm$ 10
R396E	Inactive	Inactive	Inactive	Inactive	NA	24 $\pm$ 3
W400D	Inactive	Inactive	Inactive	Inactive	NA	20 $\pm$ 2

(methylated rpS2) was quantified by tracing the radioactivity (counts per minute measured by a TopCount reader from Perkin Elmer). Assay conditions were optimized so that the experiment was performed at linear initial velocity. PRMT3, rpS2 and SAM concentrations were 500 nM, 1  $\mu\text{M}$ , and 50  $\mu\text{M}$ , respectively. The reaction was prepared in the final volume of 20  $\mu\text{l}$ . The reaction mixture contained 14  $\mu\text{l}$  of buffer (20 mM Tris, 10 mM DTT [pH 8]), 2  $\mu\text{l}$  enzyme, and 2  $\mu\text{l}$  of 66  $\mu\text{M}$   $^3\text{H}$ -SAM (diluted with cold SAM to achieve the desired SAM concentration). The reaction was started by adding 2  $\mu\text{l}$  of rpS2 substrate. The reaction mixtures were incubated for 45 min and quenched with 80  $\mu\text{l}$  10% TCA. One hundred microliters of the reaction mix containing TCA was transferred into a filter plate (96-well Multiscreen Filter Plates from Millipor). The plate was washed twice with 80  $\mu\text{l}$  10% TCA and once with ethanol. After ethanol evaporated, 50  $\mu\text{l}$  of scintillation liquid was added and radioactivity was measured using a TopCount (Perkin Elmer).

#### Crystallization

PRMT3 was incubated at 1.1 mg/ml overnight with compound **1** at 1:30 molar ratio (PRMT3: compound **1**). Following incubation, protein was concentrated to 3 mg/ml and crystallized using the sitting drop diffusion method at 20°C by mixing 1  $\mu\text{l}$  of the protein solution with 1  $\mu\text{l}$  of the reservoir solution containing 20% PEG 4K, 0.2 M MgOAc, 0.1 M NaCaco (pH 6.5). Prior to freezing, 0.1  $\mu\text{l}$

of 100 mM compound **1** was added directly to the drop. Crystals were soaked for 30 min in the same buffer with 10% glycerol.

#### Data Collection and Processing

The native data set was collected on CLS beamline CMCF-ID at 100 K. Program HKL2000 was used for data processing and scaling (Minor et al., 2006).

#### Structure Determination and Refinement

PRMT3 structure in complex with compound **1** was determined using the molecular replacement method with the 2FYT structure as a model. Graphic program COOT was used for manual model refinement and visualization (Emsley and Cowtan, 2004). Refmac5 were used to refine the model (Murshudov et al., 1997). MolProbity was used to validate the refined structure (Chen et al., 2010). Ninety eight percent of residues are in the favored regions of Ramachandran plot and none of them in the disallowed regions. The structure has been deposited in the RCSB with PDB code 3SMQ.

#### SPR Experiments

SPR experiments were performed at 25°C using a GE Healthcare Biacore T200 instrument (<http://www.biacore.com>). 6xHis-tagged PRMT3 protein (20  $\mu\text{g}/\text{ml}$

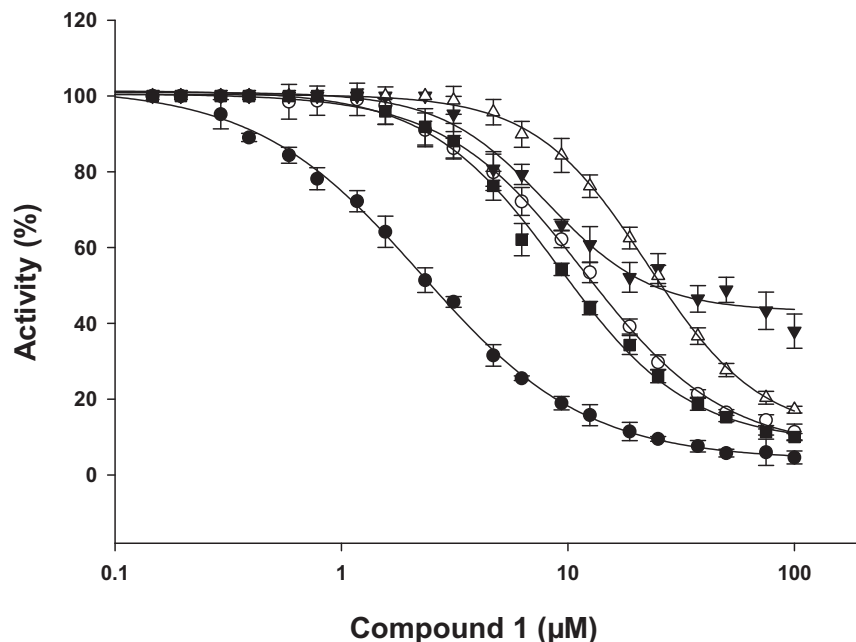
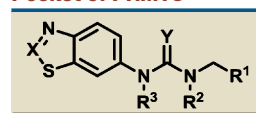


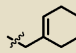
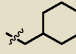
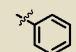
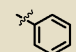
**Figure 6. Effect of Compound 1 on Activity of PRMT3 Variants**

$\text{IC}_{50}$  values were determined at balanced conditions using SAHH-coupled assay for wild-type PRMT3 ( $\bullet$ ), K392R ( $\circ$ ), E422A ( $\blacktriangledown$ ), V420W ( $\triangle$ ), and K392A ( $\blacksquare$ ). E422A was only active when freshly made and lost activity quickly, making it difficult to determine its kinetic parameters reproducibly. Therefore the experiments for this mutant were performed at estimated  $K_m$  of substrates (3  $\mu\text{M}$  of peptide and 50  $\mu\text{M}$  of SAM) for comparison. Data points are presented as mean values  $\pm$  SD from three experiments.



**Table 3. SAR of the Compounds Designed to Probe Hydrogen-Bond Interactions of Compound 1 with the Allosteric Binding Pocket of PRMT3**



Compound ID	R <sup>1</sup>	R <sup>2</sup>	R <sup>3</sup>	X	Y	PRMT3 IC <sub>50</sub> (μM)
1		H	H	N	O	2.5 ± 0.1
2		H	H	N	O	1.4 ± 0.1
3		H	H	CH	O	> 100
4		H	CH <sub>3</sub>	N	O	> 100
5		H	H	N	O	20 ± 1
6		H	H	N	S	> 100
7		CH <sub>3</sub>	H	N	O	> 100

in 10 mM sodium acetate [pH 5.0]) was amine-coupled to a CM5 chip using the GE Healthcare amine coupling kit (BR-1000-50) and the manufacturer's standard protocol (5779 RU immobilized). All small molecule analysis experiments were performed in HBS-EP running buffer (10 mM HEPES [pH 7.4], 150 mM NaCl, 3 mM EDTA, 0.05% Tween-20) supplemented with 5% DMSO. The PRMT3–compound **1** affinity determination was performed in duplicate using single cycle kinetics with a 5 point, 2-fold serial dilution from 20 μM down to 1.25 μM. A flow rate of 30 μl/minute was used with on and off times of 60 s each. A DMSO calibration curve was used for data correction. K<sub>D</sub> values were calculated using the Biacore BiaEvaluation software (GE Healthcare).

#### Isothermal Aggregation

Half-life of all mutants and the wild-type were determined using isothermal aggregation as described before (Hong et al., 2010) (Supplemental Experimental Procedures).

#### Compound Quality Control

Compounds ordered from vendors were evaluated for purity by LC/MS with an acceptable purity standard set at ≥85% by UV (254 nm). Purity (along with compound identity) was further confirmed by nuclear magnetic resonance spectroscopy (500 MHz), and compounds failing to meet the standard were subsequently purified by silica gel column chromatography prior to further assessment.

#### Chemical Synthesis

Synthetic procedures and chemical characterization of compounds **1**, **2**, **3**, **4**, **5**, **6**, and **7** are detailed in the Supplemental Experimental Procedures.

#### SUPPLEMENTAL INFORMATION

Supplemental Information includes three figures, two tables, Supplemental Experimental Procedures, and Supplemental References and can be found with this article online at <http://dx.doi.org/10.1016/j.str.2012.06.001>.

#### ACKNOWLEDGMENTS

We would like to thank Dr. Mark Bedford for providing rpS2 constructs and reviewing the related data. The Structural Genomics Consortium is a registered charity (number 1097737) that receives funds from Canadian Institutes for Health Research, Canadian Foundation for Innovation, Genome Canada through the Ontario Genomics Institute, GlaxoSmithKline, Eli Lilly, Pfizer, Novartis Research Foundation, Life Technologies, Ontario Innovation Trust,

Ontario Ministry for Research and Innovation, and Wellcome Trust. We thank the University Cancer Research Fund (UCRF) and the Carolina Partnership from the University of North Carolina at Chapel Hill for financial support. Funding for OICR is provided by the Government of Ontario.

Received: December 14, 2011

Revised: May 24, 2012

Accepted: June 2, 2012

Published online: July 12, 2012

#### REFERENCES

- Albert, M., and Helin, K. (2010). Histone methyltransferases in cancer. *Semin. Cell Dev. Biol.* *21*, 209–220.
- Allali-Hassani, A., Wasney, G.A., Siarheyeva, A., Hajian, T., Arrowsmith, C.H., and Vedadi, M. (2011). Fluorescence-Based Methods for Screening Writers and Readers of Histone Methyl Marks. *J. Biomol. Screen.*
- Allan, M., Manku, S., Therrien, E., Nguyen, N., Styhler, S., Robert, M.F., Goulet, A.C., Petschner, A.J., Rahil, G., Robert Macleod, A., et al. (2009). N-Benzyl-1-heteroaryl-3-(trifluoromethyl)-1H-pyrazole-5-carboxamides as inhibitors of co-activator associated arginine methyltransferase 1 (CARM1). *Bioorg. Med. Chem. Lett.* *19*, 1218–1223.
- Artursson, P. (1990). Epithelial transport of drugs in cell culture. I: A model for studying the passive diffusion of drugs over intestinal absorptive (Caco-2) cells. *J. Pharm. Sci.* *79*, 476–482.
- Bachand, F., and Silver, P.A. (2004). PRMT3 is a ribosomal protein methyltransferase that affects the cellular levels of ribosomal subunits. *EMBO J.* *23*, 2641–2650.
- Bedford, M.T., and Richard, S. (2005). Arginine methylation an emerging regulator of protein function. *Mol. Cell* *18*, 263–272.
- Bissinger, E.M., Heinke, R., Spannhoff, A., Eberlin, A., Metzger, E., Cura, V., Hassenboehler, P., Cavarelli, J., Schüle, R., Bedford, M.T., et al. (2011). Acyl derivatives of p-aminosulfonamides and dapsone as new inhibitors of the arginine methyltransferase hPRMT1. *Bioorg. Med. Chem.* *19*, 3717–3731.
- Brais, B., Bouchard, J.P., Xie, Y.G., Rochefort, D.L., Chrétien, N., Tomé, F.M., Lafrenière, R.G., Rommens, J.M., Uyama, E., Nohira, O., et al. (1998). Short GCG expansions in the PABP2 gene cause oculopharyngeal muscular dystrophy. *Nat. Genet.* *18*, 164–167.
- Campagna-Slater, V., Mok, M.W., Nguyen, K.T., Feher, M., Najmanovich, R., and Schapira, M. (2011). Structural chemistry of the histone methyltransferases cofactor binding site. *J. Chem. Inf. Model.* *51*, 612–623.
- Chen, V.B., Arendall, W.B., 3rd, Headd, J.J., Keedy, D.A., Immormino, R.M., Kapral, G.J., Murray, L.W., Richardson, J.S., and Richardson, D.C. (2010). MolProbity: all-atom structure validation for macromolecular crystallography. *Acta Crystallogr. D Biol. Crystallogr.* *66*, 12–21.
- Chen, X., Niroomand, F., Liu, Z., Zankl, A., Katus, H.A., Jahn, L., and Tiefenbacher, C.P. (2006). Expression of nitric oxide related enzymes in coronary heart disease. *Basic Res. Cardiol.* *101*, 346–353.
- Cheng, D., Valente, S., Castellano, S., Sbardella, G., Di Santo, R., Costi, R., Bedford, M.T., and Mai, A. (2011). Novel 3,5-bis(bromohydroxybenzylidene)pyridin-4-ones as coactivator-associated arginine methyltransferase 1 inhibitors: enzyme selectivity and cellular activity. *J. Med. Chem.* *54*, 4928–4932.
- Colasanti, M., and Suzuki, H. (2000). The dual personality of NO. *Trends Pharmacol. Sci.* *21*, 249–252.
- Copeland, R.A., Solomon, M.E., and Richon, V.M. (2009). Protein methyltransferases as a target class for drug discovery. *Nat. Rev. Drug Discov.* *8*, 724–732.
- Daigle, S.R., Olhava, E.J., Therkelsen, C.A., Majer, C.R., Sneeringer, C.J., Song, J., Johnston, L.D., Scott, M.P., Smith, J.J., Xiao, Y., et al. (2011). Selective killing of mixed lineage leukemia cells by a potent small-molecule DOT1L inhibitor. *Cancer Cell* *20*, 53–65.
- Dhayalan, A., Kudithipudi, S., Rathert, P., and Jeltsch, A. (2011). Specificity analysis-based identification of new methylation targets of the SET7/9 protein lysine methyltransferase. *Chem. Biol.* *18*, 111–120.

- Di Lorenzo, A., and Bedford, M.T. (2011). Histone arginine methylation. *FEBS Lett.* **585**, 2024–2031.
- El Messaoudi, S., Fabbriozzi, E., Rodriguez, C., Chuchana, P., Fauquier, L., Cheng, D., Theillet, C., Vandel, L., Bedford, M.T., and Sardet, C. (2006). Coactivator-associated arginine methyltransferase 1 (CARM1) is a positive regulator of the Cyclin E1 gene. *Proc. Natl. Acad. Sci. USA* **103**, 13351–13356.
- Emsley, P., and Cowtan, K. (2004). Coot: model-building tools for molecular graphics. *Acta Crystallogr. D Biol. Crystallogr.* **60**, 2126–2132.
- Engman, H.A., Lennernäs, H., Taipalensuu, J., Otter, C., Leidvik, B., and Artursson, P. (2001). CYP3A4, CYP3A5, and MDR1 in human small and large intestinal cell lines suitable for drug transport studies. *J. Pharm. Sci.* **90**, 1736–1751.
- Ferguson, A.D., Larsen, N.A., Howard, T., Pollard, H., Green, I., Grande, C., Cheung, T., Garcia-Arenas, R., Cowen, S., Wu, J., et al. (2011). Structural basis of substrate methylation and inhibition of SMYD2. *Structure* **19**, 1262–1273.
- Frietze, S., Lupien, M., Silver, P.A., and Brown, M. (2008). CARM1 regulates estrogen-stimulated breast cancer growth through up-regulation of E2F1. *Cancer Res.* **68**, 301–306.
- Fronz, K., Otto, S., Köbel, K., Kühn, U., Friedrich, H., Schierhorn, A., Beck-Sickingler, A.G., Ostareck-Lederer, A., and Wahle, E. (2008). Promiscuous modification of the nuclear poly(A)-binding protein by multiple protein-arginine methyltransferases does not affect the aggregation behavior. *J. Biol. Chem.* **283**, 20408–20420.
- Groop, P.H., Forsblom, C., and Thomas, M.C. (2005). Mechanisms of disease: Pathway-selective insulin resistance and microvascular complications of diabetes. *Nature Clin. Pract.* **1**, 100–110.
- Guccione, E., Bassi, C., Casadio, F., Martinato, F., Cesaroni, M., Schuchlantz, H., Lüscher, B., and Amati, B. (2007). Methylation of histone H3R2 by PRMT6 and H3K4 by an MLL complex are mutually exclusive. *Nature* **449**, 933–937.
- Herrmann, F., Pably, P., Eckerich, C., Bedford, M.T., and Fackelmayer, F.O. (2009). Human protein arginine methyltransferases in vivo—distinct properties of eight canonical members of the PRMT family. *J. Cell Sci.* **122**, 667–677.
- Hong, B.S., Allali-Hassani, A., Tempel, W., Finerty, P.J., Jr., Mackenzie, F., Dimov, S., Vedadi, M., and Park, H.W. (2010). Crystal structures of human choline kinase isoforms in complex with hemicholinium-3: single amino acid near the active site influences inhibitor sensitivity. *J. Biol. Chem.* **285**, 16330–16340.
- Hong, H., Kao, C., Jeng, M.H., Eble, J.N., Koch, M.O., Gardner, T.A., Zhang, S., Li, L., Pan, C.X., Hu, Z., et al. (2004). Aberrant expression of CARM1, a transcriptional coactivator of androgen receptor, in the development of prostate carcinoma and androgen-independent status. *Cancer* **101**, 83–89.
- Huang, J., Dorsey, J., Chuikov, S., Pérez-Burgos, L., Zhang, X., Jenuwein, T., Reinberg, D., and Berger, S.L. (2010). G9a and Glp methylate lysine 373 in the tumor suppressor p53. *J. Biol. Chem.* **285**, 9636–9641.
- Huynh, T., Chen, Z., Pang, S., Geng, J., Bandiera, T., Bindi, S., Vianello, P., Roletto, F., Thieffine, S., Galvani, A., et al. (2009). Optimization of pyrazole inhibitors of Coactivator Associated Arginine Methyltransferase 1 (CARM1). *Bioorg. Med. Chem. Lett.* **19**, 2924–2927.
- Hyllus, D., Stein, C., Schnabel, K., Schiltz, E., Imhof, A., Dou, Y., Hsieh, J., and Bauer, U.M. (2007). PRMT6-mediated methylation of R2 in histone H3 antagonizes H3 K4 trimethylation. *Genes Dev.* **21**, 3369–3380.
- Iberg, A.N., Espejo, A., Cheng, D., Kim, D., Michaud-Levesque, J., Richard, S., and Bedford, M.T. (2008). Arginine methylation of the histone H3 tail impedes effector binding. *J. Biol. Chem.* **283**, 3006–3010.
- Kelly, T.K., De Carvalho, D.D., and Jones, P.A. (2010). Epigenetic modifications as therapeutic targets. *Nat. Biotechnol.* **28**, 1069–1078.
- Kielstein, J.T., Bode-Böger, S.M., Frölich, J.C., Haller, H., and Böger, R.H. (2001a). Relationship of asymmetric dimethylarginine to dialysis treatment and atherosclerotic disease. *Kidney Int. Suppl.* **78**, S9–S13.
- Kielstein, J.T., Frölich, J.C., Haller, H., and Fliser, D. (2001b). ADMA (asymmetric dimethylarginine): an atherosclerotic disease mediating agent in patients with renal disease? *Nephrol. Dial. Transplant.* **16**, 1742–1745.
- Liu, X., Wang, D., Zhao, Y., Tu, B., Zheng, Z., Wang, L., Wang, H., Gu, W., Roeder, R.G., and Zhu, W.G. (2011). Methyltransferase Set7/9 regulates p53 activity by interacting with Sirtuin 1 (SIRT1). *Proc. Natl. Acad. Sci. USA* **108**, 1925–1930.
- Mariotto, S., Menegazzi, M., and Suzuki, H. (2004). Biochemical aspects of nitric oxide. *Curr. Pharm. Des.* **10**, 1627–1645.
- Meyer, R.P., Gehlhaus, M., Knoth, R., and Volk, B. (2007). Expression and function of cytochrome p450 in brain drug metabolism. *Curr. Drug Metab.* **8**, 297–306.
- Minor, W., Cymborowski, M., Otwinowski, Z., and Chruszcz, M. (2006). HKL-3000: the integration of data reduction and structure solution—from diffraction images to an initial model in minutes. *Acta Crystallogr.* **62**, 859–866.
- Miyata, S., Mori, Y., and Tohyama, M. (2010). PRMT3 is essential for dendritic spine maturation in rat hippocampal neurons. *Brain Res.* **1352**, 11–20.
- Murshudov, G.N., Vagin, A.A., and Dodson, E.J. (1997). Refinement of macromolecular structures by the maximum-likelihood method. *Acta Crystallogr. D Biol. Crystallogr.* **53**, 240–255.
- Nimura, K., Ura, K., and Kaneda, Y. (2010). Histone methyltransferases: regulation of transcription and contribution to human disease. *J. Mol. Med.* **88**, 1213–1220.
- Obianyo, O., Causey, C.P., Jones, J.E., and Thompson, P.R. (2011). Activity-based protein profiling of protein arginine methyltransferase 1. *ACS Chem Biol.* **6**, 1127–1135.
- Pagans, S., Kauder, S.E., Kaehlicke, K., Sakane, N., Schroeder, S., Dormeyer, W., Trievel, R.C., Verdin, E., Schnolzer, M., and Ott, M. (2010). The Cellular lysine methyltransferase Set7/9-KMT7 binds HIV-1 TAR RNA, monomethylates the viral transactivator Tat, and enhances HIV transcription. *Cell Host Microbe* **7**, 234–244.
- Pawlak, M.R., Scherer, C.A., Chen, J., Roshon, M.J., and Ruley, H.E. (2000). Arginine N-methyltransferase 1 is required for early postimplantation mouse development, but cells deficient in the enzyme are viable. *Mol. Cell Biol.* **20**, 4859–4869.
- Petrossian, T.C., and Clarke, S.G. (2011). Uncovering the human methyltransferasome. *Mol. Cell. Proteomics* **10**, M110.000976.
- Purandare, A.V., Chen, Z., Huynh, T., Pang, S., Geng, J., Vaccaro, W., Poss, M.A., Oconnell, J., Nowak, K., and Jayaraman, L. (2008). Pyrazole inhibitors of coactivator associated arginine methyltransferase 1 (CARM1). *Bioorg. Med. Chem. Lett.* **18**, 4438–4441.
- Richon, V.M., Johnston, D., Sneeringer, C.J., Jin, L., Majer, C.R., Elliston, K., Jerva, L.F., Scott, M.P., and Copeland, R.A. (2011). Chemogenetic analysis of human protein methyltransferases. *Chem. Biol.* **20**, 199–210.
- Sack, J.S., Thieffine, S., Bandiera, T., Fasolini, M., Duke, G.J., Jayaraman, L., Kish, K.F., Klei, H.E., Purandare, A.V., Rosettani, P., et al. (2011). Structural basis for CARM1 inhibition by indole and pyrazole inhibitors. *Biochem. J.* **436**, 331–339.
- Shi, X., Kachirskaia, I., Yamaguchi, H., West, L.E., Wen, H., Wang, E.W., Dutta, S., Appella, E., and Gozani, O. (2007). Modulation of p53 function by SET8-mediated methylation at lysine 382. *Mol. Cell* **27**, 636–646.
- Singh, V., Miranda, T.B., Jiang, W., Frankel, A., Roemer, M.E., Robb, V.A., Gutmann, D.H., Herschman, H.R., Clarke, S., and Newsham, I.F. (2004). DAL-1/4.1B tumor suppressor interacts with protein arginine N-methyltransferase 3 (PRMT3) and inhibits its ability to methylate substrates in vitro and in vivo. *Oncogene* **23**, 7761–7771.
- Smith, J.J., Rücknagel, K.P., Schierhorn, A., Tang, J., Nemeth, A., Linder, M., Herschman, H.R., and Wahle, E. (1999). Unusual sites of arginine methylation in Poly(A)-binding protein II and in vitro methylation by protein arginine methyltransferases PRMT1 and PRMT3. *J. Biol. Chem.* **274**, 13229–13234.
- Swanson, H.I. (2004). Cytochrome P450 expression in human keratinocytes: an aryl hydrocarbon receptor perspective. *Chem. Biol. Interact.* **149**, 69–79.
- Swiercz, R., Person, M.D., and Bedford, M.T. (2005). Ribosomal protein S2 is a substrate for mammalian PRMT3 (protein arginine methyltransferase 3). *Biochem. J.* **386**, 85–91.
- Swiercz, R., Cheng, D., Kim, D., and Bedford, M.T. (2007). Ribosomal protein rpS2 is hypomethylated in PRMT3-deficient mice. *J. Biol. Chem.* **282**, 16917–16923.

- Tang, J., Gary, J.D., Clarke, S., and Herschman, H.R. (1998). PRMT 3, a type I protein arginine N-methyltransferase that differs from PRMT1 in its oligomerization, subcellular localization, substrate specificity, and regulation. *J. Biol. Chem.* **273**, 16935–16945.
- Tavanez, J.P., Bengoechea, R., Berciano, M.T., Lafarga, M., Carmo-Fonseca, M., and Enguita, F.J. (2009). Hsp70 chaperones and type I PRMTs are sequestered at intranuclear inclusions caused by polyalanine expansions in PABPN1. *PLoS ONE* **4**, e6418.
- Therrien, E., Larouche, G., Manku, S., Allan, M., Nguyen, N., Styhler, S., Robert, M.F., Goulet, A.C., Besterman, J.M., Nguyen, H., and Wahhab, A. (2009). 1,2-Diamines as inhibitors of co-activator associated arginine methyltransferase 1 (CARM1). *Bioorg. Med. Chem. Lett.* **19**, 6725–6732.
- Troffer-Charlier, N., Cura, V., Hassenboehler, P., Moras, D., and Cavarelli, J. (2007). Functional insights from structures of coactivator-associated arginine methyltransferase 1 domains. *EMBO J.* **26**, 4391–4401.
- Vallance, P., and Leiper, J. (2004). Cardiovascular biology of the asymmetric dimethylarginine:dimethylarginine dimethylaminohydrolase pathway. *Arterioscler. Thromb. Vasc. Biol.* **24**, 1023–1030.
- Vedadi, M., Barsyte-Lovejoy, D., Liu, F., Rival-Gervier, S., Allali-Hassani, A., Labrie, V., Wigle, T.J., Dimaggio, P.A., Wasney, G.A., Siarheyeva, A., et al. (2011). A chemical probe selectively inhibits G9a and GLP methyltransferase activity in cells. *Nat. Chem. Biol.* **7**, 566–574.
- Wagner, S., Weber, S., Kleinschmidt, M.A., Nagata, K., and Bauer, U.M. (2006). SET-mediated promoter hypoacetylation is a prerequisite for coactivation of the estrogen-responsive pS2 gene by PRMT1. *J. Biol. Chem.* **281**, 27242–27250.
- Wan, H., Huynh, T., Pang, S., Geng, J., Vaccaro, W., Poss, M.A., Trainor, G.L., Lorenzi, M.V., Gottardis, M., Jayaraman, L., and Purandare, A.V. (2009). Benzo [d]imidazole inhibitors of Coactivator Associated Arginine Methyltransferase 1 (CARM1)—Hit to Lead studies. *Bioorg. Med. Chem. Lett.* **19**, 5063–5066.
- Wu, H., Min, J., Lunin, V.V., Antoshenko, T., Dombrovski, L., Zeng, H., Allali-Hassani, A., Campagna-Slater, V., Vedadi, M., Arrowsmith, C.H., et al. (2010). Structural biology of human H3K9 methyltransferases. *PLoS ONE* **5**, e8570.
- Yadav, N., Lee, J., Kim, J., Shen, J., Hu, M.C., Aldaz, C.M., and Bedford, M.T. (2003). Specific protein methylation defects and gene expression perturbations in coactivator-associated arginine methyltransferase 1-deficient mice. *Proc. Natl. Acad. Sci. USA* **100**, 6464–6468.
- Yamagishi, S., and Matsui, T. (2011). Nitric oxide, a janus-faced therapeutic target for diabetic microangiopathy—Friend or foe? *Pharmacol. Res.* **64**, 187–194.
- Yee, S. (1997). In vitro permeability across Caco-2 cells (colonic) can predict in vivo (small intestinal) absorption in man—fact or myth. *Pharm. Res.* **14**, 763–766.
- Yoshimatsu, M., Toyokawa, G., Hayami, S., Unoki, M., Tsunoda, T., Field, H.I., Kelly, J.D., Neal, D.E., Maehara, Y., Ponder, B.A., et al. (2011). Dysregulation of PRMT1 and PRMT6, Type I arginine methyltransferases, is involved in various types of human cancers. *Int. J. Cancer* **128**, 562–573.
- Yost, J.M., Korboukh, I., Liu, F., Gao, C., and Jin, J. (2011). Targets in epigenetics: inhibiting the methyl writers of the histone code. *Curr. Chem. Genomics* **5**, 72–84.
- Yue, W.W., Hassler, M., Roe, S.M., Thompson-Vale, V., and Pearl, L.H. (2007). Insights into histone code syntax from structural and biochemical studies of CARM1 methyltransferase. *EMBO J.* **26**, 4402–4412.
- Zhang, X., and Cheng, X. (2003). Structure of the predominant protein arginine methyltransferase PRMT1 and analysis of its binding to substrate peptides. *Structure* **11**, 509–520.
- Zhang, X., Zhou, L., and Cheng, X. (2000). Crystal structure of the conserved core of protein arginine methyltransferase PRMT3. *EMBO J.* **19**, 3509–3519.
- Zurita-Lopez, C.I., Sandberg, T., Kelly, R., and Clarke, S.G. (2012). Human protein arginine methyltransferase 7 (PRMT7) is a type III enzyme forming  $\omega$ -NG-monomethylated arginine residues. *J. Biol. Chem.* **287**, 7859–7870.